

Synthesis and Characterization of Bismuth Tantalate Binary Materials for Potential Application in Multilayer Ceramic Capacitors (MLCC)

K.B. Tan*, F.G. Anna and Z. Zainal

Chemistry Department, Faculty of Science, Universiti Putra Malaysia,
43400 Serdang, Malaysia

*Corresponding author: tankb@science.upm.edu.my

Abstract: *The single phase bismuth tantalate (BiTaO_4) was successfully synthesized by conventional solid-state method at sintering temperature 1100°C . This material crystallized in a triclinic system, space group $P\bar{1}$ with $a = 7.6585 \text{ \AA}$, $b = 5.5825 \text{ \AA}$, $c = 7.7795 \text{ \AA}$, $\alpha = 90.03^\circ$, $\beta = 77.04^\circ$ and $\gamma = 86.48^\circ$, respectively. The electrical properties of BiTaO_4 were characterized by AC impedance analyzer, HP4192 at temperature ranging from 25°C – 850°C over frequency range of 5–13 MHz. The sample was highly resistive as the conductivities were unlikely to be determined below 550°C . On the other hand, BiTaO_4 exhibited moderate dielectric constant, $\epsilon_r = 47$ at ambient temperature in the frequency region of 1 MHz and near zero temperature coefficient of capacitance (TCC), 0.00022, making it a potential candidate for multilayer ceramic capacitors (MLCC).*

Keywords: solid-state method, electroceramics, dielectric constant, AC impedance spectroscopy

Abstrak: *Fasa tunggal bismut tantalat (BiTaO_4) telah disintesis secara kaedah keadaan pepejal pada suhu 1100°C . Bahan ini berkrystal dalam sistem triklinik, kumpulan ruang $P\bar{1}$ dengan $a = 7.6585 \text{ \AA}$, $b = 5.5825 \text{ \AA}$, $c = 7.7795 \text{ \AA}$, $\alpha = 90.03^\circ$, $\beta = 77.04^\circ$ dan $\gamma = 86.48^\circ$. Sifat elektrik telah dikaji dengan penggunaan impedans AC, HP4192 dalam lingkungan suhu 25°C – 850°C daripada frekuensi 5–13 MHz. Sampel ini mempunyai kerintangan yang tinggi, dan kekonduksian adalah tidak mungkin ditentukan pada suhu bawah 550°C . Sementara itu, BiTaO_4 menunjukkan pemalar dielektrik, $\epsilon_r = 47$ pada suhu sekitar dalam frekuensi 1 MHz dan juga pekali suhu bagi kapasitans (TCC), 0.00022 menyebabkan kesesuaian dijadikan sebagai kapasitor seramik berlapisan (MLCC).*

Kata kunci: kaedah keadaan pepejal, elektroseramik, pemalar dielektrik, spektroskopi impedans AC

1. INTRODUCTION

Bismuth derivatives have received tremendous research interests due to their technological importance in various applications ranging from oxide ion

conductors, catalysts, band-pass filters, radio frequency applications and others.¹⁻⁵ The interesting properties are anticipated at the helm of bismuth powder due to its volatile, reactive characteristic and relatively low firing temperature in forming binary or ternary materials with other elements, e.g. bismuth vanadates, bismuth niobates or even structurally complex Bi-based pyrochlores.³⁻⁷ However, functionality of these advanced ceramics always relies on compositional variation, control and processing that require better understanding through knowledge advancement in multi-disciplinary.

Long gone are the days of integrating active or passive components onto the substrate using conventional printed circuit board (PCB) technique, which tends to be replaced by multilayer ceramic technology. This satisfies the trend of miniaturization and high functionality of modern electronic devices as green ceramic tapes of different materials serving different passive functions are laminated and co-fired at a lower firing temperature.⁸ Therefore, compatibility of desired materials with electrodes, in particularly low melting temperature silver or gold electrode is of utmost attention prior to prototype testing or commercial applications. Of particular interest in electroceramics is bismuth based dielectrics which possess low-firing temperature; and have been extensively studied for MLCC.^{5,9-10} Previous works have shown that, BiTaO₄ is a good dielectric material with high dielectric constant, high $Q \times f$ values and a near zero temperature coefficient of resonant frequency. In general, BiTaO₄ originates from ABO₄ family of compounds ($A = \text{Bi}^{3+}$ or Sb^{3+} , and $B = \text{Nb}^{5+}$, Ta^{5+} or Sb^{5+}) with the stibiotantalite structure $\text{Sb}(\text{Ta},\text{Nb})\text{O}_4$ that consists of layers of vertex sharing, distorted BO₆ octahedral parallel to the (001) plane of the orthorhombic unit cell.¹¹ At low temperature, BiTaO₄ adopted crystal orthorhombic structure similar to that of SbTaO₄ type and then transformed into triclinic phase at temperature above 870°C.¹⁰ The present study focused on the phase formation, thermal and electrical properties of BiTaO₄ phase using combination techniques including AC impedance spectroscopy, differential thermal analysis (DTA) and thermal gravimetric analysis (TGA).

2. EXPERIMENTAL

The BiTaO₄ was prepared via conventional solid-state reaction using Bi₂O₃ (Alfa Aesar, 99.99%) and Ta₂O₅ (Alfa Aesar, 99.99%) as starting materials. Prior to weighting, both Bi₂O₃ and Ta₂O₅ were dried for 3 h at 300°C and 600°C, respectively. Stoichiometric quantities of the oxides were weighted and mixed with sufficient acetone in an agate mortar to ensure the homogeneity of the mixture. The resulting powder was transferred into a platinum boat and pre-fired at 400°C and 600°C for 2 h in a Carbolite muffle furnace before firing overnight at 800°C. Subsequently, the mixture was fired at temperatures of

1000°C and 1100°C for 24 h with intermediate regrinding. The phase purity of the sample was examined at room temperature by X-ray diffraction (XRD) using Shimadzu X-ray powder diffractometer XRD-6000, which was equipped with a diffracted-beam graphite monochromator, with $\text{CuK}\alpha$ radiation (1.5418×10^{-10} m). Pellets of single phase sample were prepared using a stainless steel die measuring 8 mm in diameter. Sufficient amount of powder was added, cold pressed uniaxially, and sintered at 1100°C in order to increase their mechanical strength and to reduce the intergranular resistance in the pellets. Gold paste (Engelhard) was smeared and hardened onto parallel faces of the ceramics. The pellets with gold electrode attached were placed on a conductivity jig and inserted in a horizontal tube furnace. The pellets were characterized using an AC impedance analyzer, Hewlett Packard LF HP4192A over a frequency range of 5 to 13 MHz with an applied voltage of 100 mV. Conductivity measurements were carried out over the temperature range of $\sim 28^\circ\text{C}$ to 850°C on heating and cooling cycles at each 50°C interval. The samples were allowed to equilibrate at each temperature for 30 min prior to measurement.

3. RESULTS AND DISCUSSION

3.1 XRD and Thermal Analysis

BiTaO_4 powder was successfully synthesized using the conventional solid-state method. The phase of pure BiTaO_4 was obtained with final firing temperature at 1100°C after 24 h. Figure 1 shows XRD patterns of BiTaO_4 which is in good agreement with those reported in the ICDD card number 16-906. All the reflection planes in the XRD patterns are fully indexed in the triclinic system with space group $\text{P}\bar{1}$. The refined lattice parameters were: $a = 7.6585 \text{ \AA}$, $b = 5.5825 \text{ \AA}$, $c = 7.7795 \text{ \AA}$, $\alpha = 90.03^\circ$, $\beta = 77.04^\circ$, $\gamma = 86.48^\circ$ and $Z = 4$, respectively. The DTA thermogram of the BiTaO_4 recorded at a scan rate of $10^\circ\text{C min}^{-1}$ is shown in Figure 2. A reversible thermal event was discernable with endothermic and exothermic peaks at temperature 751.1°C and 673.3°C , respectively. This is probably associated with the transformation of orthorhombic $\alpha\text{-BiTaO}_4$ into triclinic $\beta\text{-BiTaO}_4$ structure.¹² Figure 3 illustrates the TGA thermogram of BiTaO_4 which is recorded from room temperature to 1000°C . However, TGA was not capable of detecting thermal event that do not involve weight change, e.g. polymorphic transition in this case.

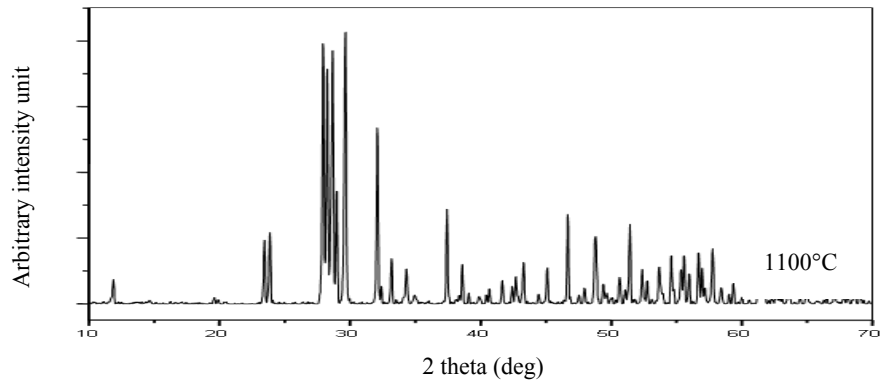


Figure 1: XRD diffraction patterns of BiTaO₄ prepared at 1100°C for 24 h.

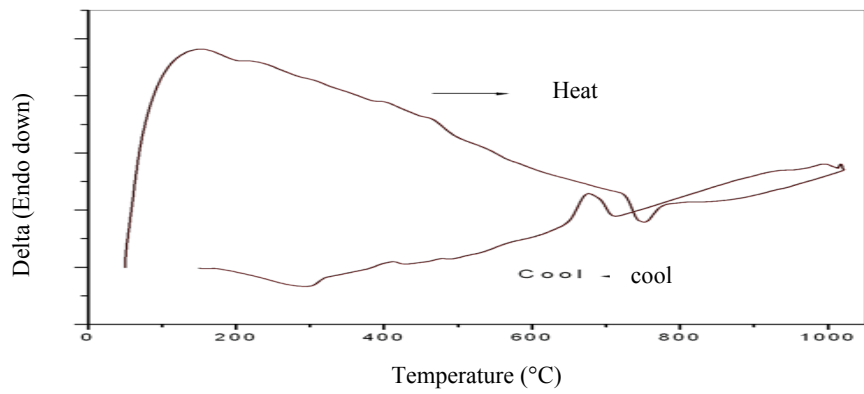


Figure 2: Differential thermal analysis thermogram of BiTaO₄.

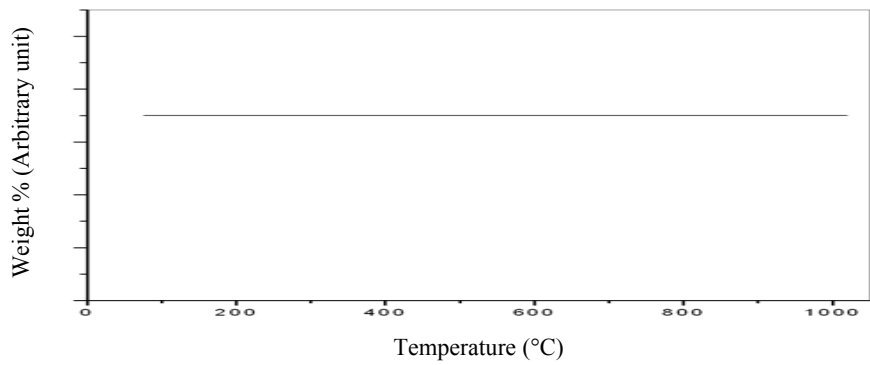


Figure 3: Thermal gravimetric analysis thermogram of BiTaO₄.

3.2 Electrical Properties

The AC impedance spectroscopy technique was applied to evaluate and separate the contribution to the overall electrical properties, of the various components such as bulk, grain-boundary or polarization phenomenon in a material.¹³ Figure 4 shows the complex impedance plot of Z'' versus Z' for BiTaO_4 at 550°C . A single perfect semicircle is only observed at temperature above 550°C . The complex plane representation shows a single non-depressed semicircle, which corresponds to a single Debye response. The high frequency semicircle represents the bulk (grain) property of the material arising due to the parallel combination of bulk resistance (R_b) and bulk capacitance (C_b) of the material. The capacitance of the sample is about $6.2794 \times 10^{-12} \text{ F cm}^{-1}$, indicating a bulk response with a permittivity of about 47–48.¹⁴ The corresponding R_b of $\sim 2.28 \times 10^6$ to $\sim 1 \times 10^4$ ohm cm over the temperature range of 550°C to 850°C are obtained from the intercept on the real part of impedance, Z' . On the other hand, TCC of BiTaO_4 is determined to be 0.00022 at temperature range of 25°C to 200°C .

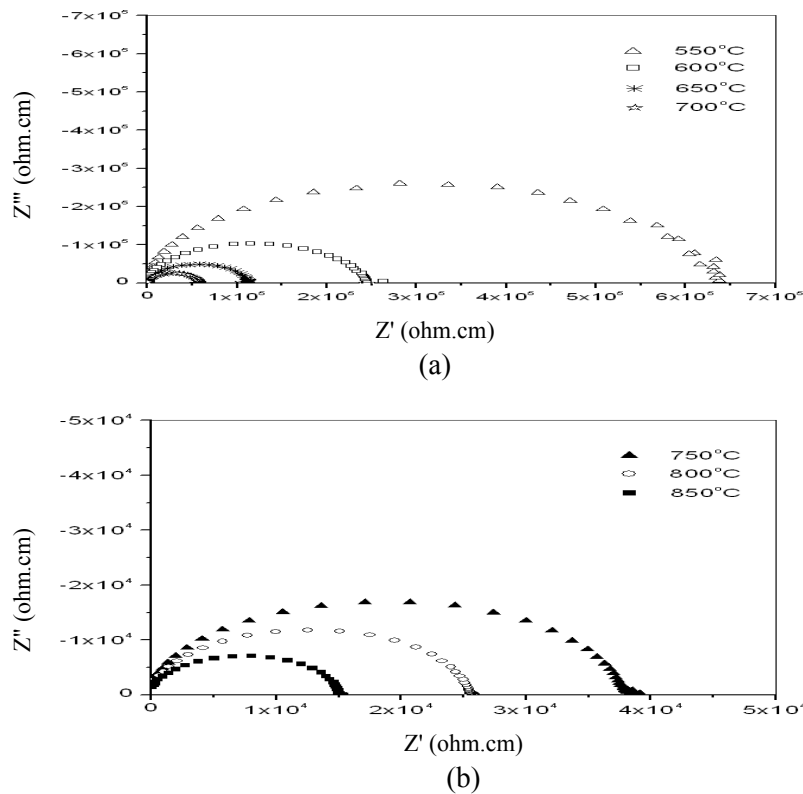


Figure 4: Cole-cole plots of BiTaO_4 at temperature range of 550°C to 850°C .

The electric modulus is proportional to C^{-1} , C being the capacitance. The peak heights of the modulus plots (Fig. 5) are independent of temperature indicating that BiTaO₄ do not exhibit ferroelectric properties in the temperature range studied. The frequency range at around the peak indicates the transition from short-range to long-range mobility of charge carriers with decreasing frequency. The peak at the relaxation is defined by the condition $\omega\tau = 1$; where τ is the most probable relaxation time.¹⁵

Figure 6 shows the electrical conductivity of the material as a function of temperature. The Arrhenius's law is applied to correlate the observed behavior with a general relation, $\sigma = \sigma_0 \exp(-E_a/kT)$ where σ_0 represents a pre-exponential factor, E_a is the apparent activation energy of the conduction process, k is Boltzmann's constant and T is the absolute temperature. The conductivity data is reproducible and reversible in heat-cool cycles, showing a good linearity over the temperature range studied. The activation energy (E_a) of the material in AC conduction is estimated to be ~ 1.04 eV from the slope of graph. The electrical homogeneity of the ceramic is confirmed by the presence of single, Debye-like peaks occurring at similar frequencies in spectroscopic plots of the imaginary components of the impedance (Z'') and electric modulus (M''), as shown in Figure 7. The frequency maxima of Z'' and M'' should be coincident, and the full width at half maximum (FWHM) should be equal to 1.14 decade for an ideal Debye response representing bulk properties. There appears to be no grain boundary effect as two overlapping peaks with FWHM value of $M'' \sim 1.33$ decade is obtained, indicating that the material is homogeneous.

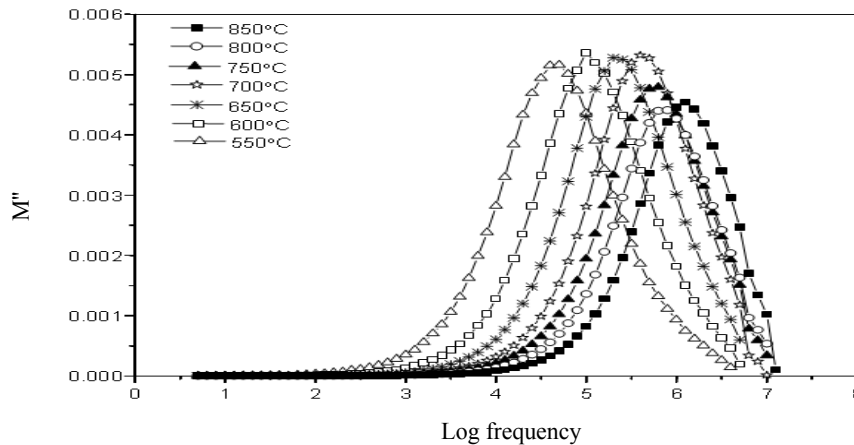


Figure 5: Imaginary part of electrical modulus as a function of frequency.

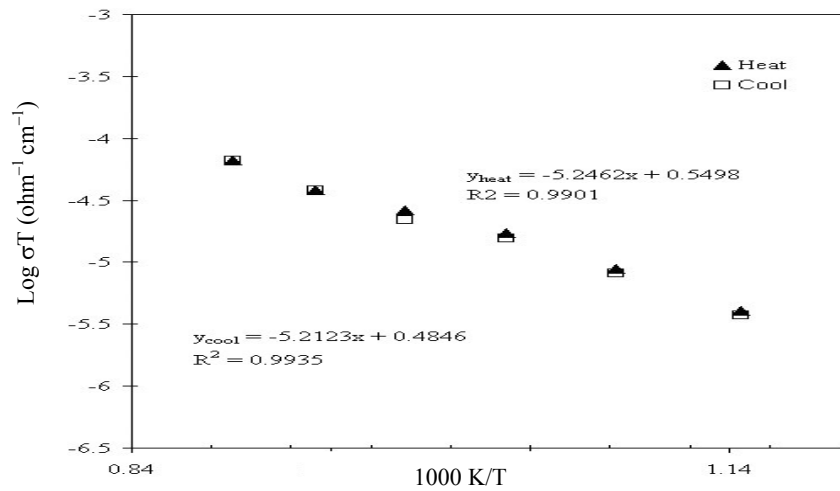


Figure 6: Conductivity Arrhenius plots of BiTaO₄.

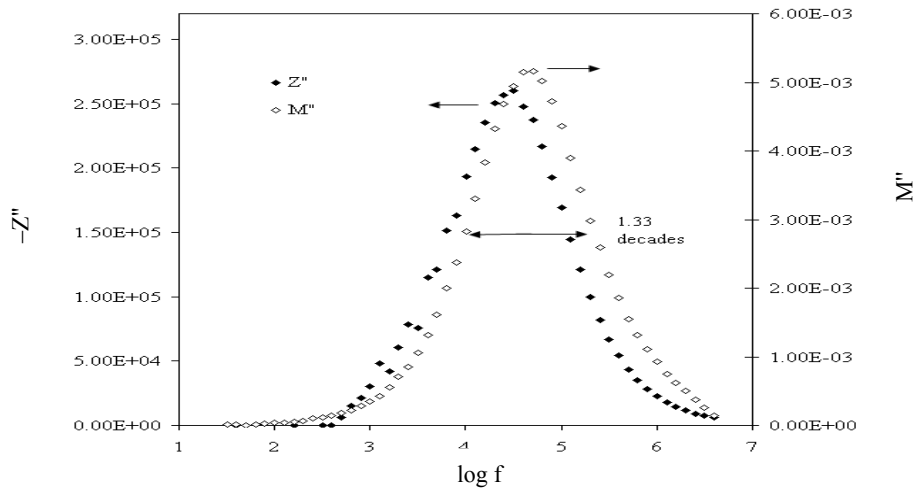


Figure 7: Combined Z'' and M'' spectroscopic plots for BiTaO₄ at 550°C.

A dispersion of Z'' as a function of frequency is shown in Figure 8. The maxima of the curves shift towards higher frequency region with the increase of measuring temperature; this indicates the presence of polarization process in the dielectric material.¹⁵ The broadening of the peaks with increasing temperatures suggest that the relaxation process is of temperature-dependent. The relaxation process that occurs in the material may probably associate with immobile species (electrons) at low temperature and defects (vacancies) at higher temperature.¹⁶

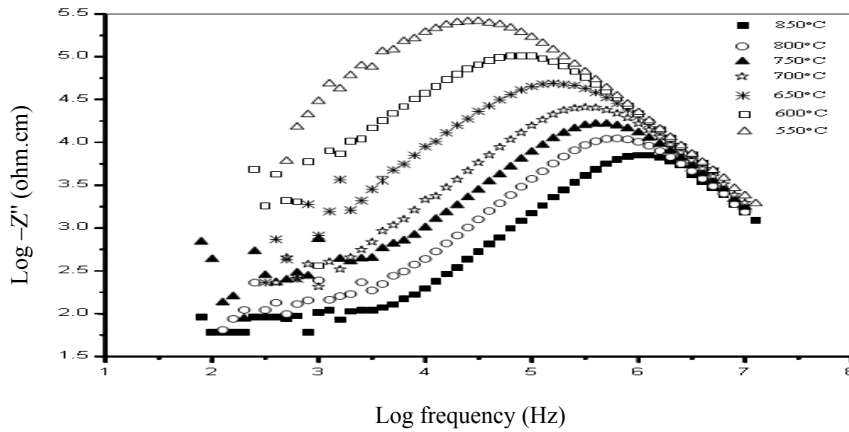


Figure 8: Imaginary part of impedance as a function of frequency for BiTaO₄ at various temperatures.

Figure 9 shows the plots of real part of complex permittivity of BiTaO₄ ceramics as a function of sintering temperature. The ϵ_r increases appreciably with the increase of temperature. The temperature dependence of ϵ_r is due to a polarization effect. The number of space-charge carrier governs the space-charge polarization. As temperature increases, electrical conductivity increases due to the increase in thermally activated drift mobility of electric charge carriers probably according to hopping conduction mechanism. Hence, the dielectric polarization increases and leads to higher ϵ_r .⁷ The dielectric dispersion is significant at higher temperatures and low frequencies. However, the lack of strong dispersion in the ϵ_r at high frequencies suggests that this phenomenon is coupled with space charge effect. Figure 10 shows the dielectric loss ($\tan \delta$) as a function of temperature for BiTaO₄ at different frequencies. It is observed that $\tan \delta$ of BiTaO₄ is independent of temperatures ranging from 25°C–500°C. All the curves display a similar behavior at temperatures below 500°C; however, at temperatures above 500°C, a slightly increased loss is observed for the three frequencies measured. No obvious dielectric peak is discernable in this temperature range. The increased $\tan \delta$ is probably attributed to the enhanced space charge relaxation due to the increase of oxygen vacancies concentration or related to the lattice vibrations at higher temperatures.

4. CONCLUSION

The BiTaO₄ was synthesized via solid-state reaction at 1100°C, with lattice parameters, $a = 7.6585 \text{ \AA}$, $b = 5.5825 \text{ \AA}$, $c = 7.7795 \text{ \AA}$, $\alpha = 90.03^\circ$, $\beta = 77.04^\circ$ and $\gamma = 86.48^\circ$, respectively. A reversible thermal event in temperature

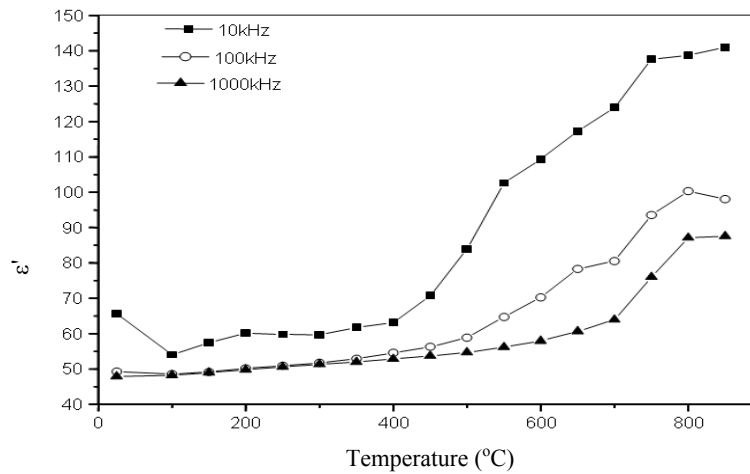


Figure 9: Real part of complex permittivity as a function of sintering temperature at several frequencies.

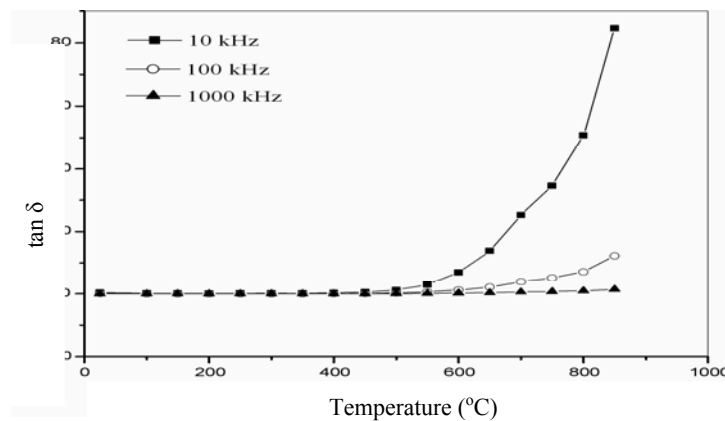


Figure 10: Dielectric losses, $\tan \delta$, as a function of sintering temperature at several frequencies .

range 600°C–800°C was observed in DTA thermogram, indicating a structural transformation occurred within the structure. On the other hand, TGA confirmed that there was no evidence of deleterious bismuth loss. The BiTaO₄ was highly resistive with R_b of $\sim 2.28 \times 10^6$ to $\sim 1 \times 10^4$ ohm cm, high activation energy in AC conduction of 1.0408 eV over the temperature range of 550°C to 850°C. The BiTaO₄ exhibited high ϵ_r , low $\tan \delta$ and near zero TCC with value of 47–48, 0.0122 and 0.00022, respectively.

5. REFERENCES

1. Lee, C.K. & West, A.R. (1996). Thermal behaviour and polymorphism of BIMEVOX oxide ion conductors including the new materials: Bi₄V₂O₁₁: M; M = La, Y, Mg, B. *Solid State Ionics*, 86–88, 235–239.
2. Okuyama, M., Wu, W.B, Oishi, Y. & Kanashima, T. (1997). Dielectric property of ferroelectric–insulator–semiconductor junction. *Appl. Surf. Sci.*, 17–118, 406–412.
3. Radosavljevic, I., Evans, J.S.O. & Sleight, A.W. (1998). Synthesis and structure of BiCa₂VO₆. *J. Solid State Chem.*, 137(1), 143–147.
4. Veen, A.C.V., Farrusseng, D., Rebeilleau, M., Decamp, T., Holzworth, A., Schuurman, Y. & Mirodatos, C. (2003). Acceleration in catalyst development by fast transient kinetic investigation. *J. Catal.*, 216(1–2), 35–143.
5. Cann, D.P., Randall, C.A. & ShROUT, T.R. (1996). Investigation of the dielectric properties of bismuth pyrochlores. *Solid State Commun.*, 100, 529–34.
6. Tan, K.B., Lee, C.K., Zainal, Z., Miles G.C. & West, A.R. (2005). Stoichiometry and doping mechanism of the cubic pyrochlore phase in the system Bi₂O₃–ZnO–Nb₂O₅. *J. Mater. Chem.*, 15, 3501–3506.
7. Khaw, C.C., Lee, C.K., Zainal, Z., Miles, G.C. & West, A.R. (2007). Pyrochlore phase formation in the system Bi₂O₃–ZnO–Ta₂O₃. *J. Am. Ceramic Soc.*, 90(9), 2900–2904.
8. Radha, R., Muthurajan, H., Koteswara Rao, N., Pradhan, S., Gupta, U.N., Jha, R.K., Mirji, S.A & Ravi, V. (2008). Low temperature synthesis and characterization of BiNbO₄ powders. *Mater. Charact.*, 59(8), 1083–1087.
9. Huang, C.L. & Weng, M.H. (2000). Low-fire BiTaO₄ dielectric ceramics for microwave applications. *Mater. Lett.*, 43, 32–35.
10. Lee, C.Y., Macquart, R., Zhou, Q. & Kennedy, B.J. (2003). Structural and spectroscopic studies of BiTa_{1-x}Nb_xO₄. *J. Solid State Chem.*, 174, 310–318.
11. Keve, E.T. & Skapski, A.C. (1973). The crystal structure of triclinic β-BiNbO₄. *J. Solid State Chem.*, 8, 159–165.
12. Subramanian, M.A. & Calibrese, J.C. (1993). Crystal structure of the low temperature form of bismuth niobium oxide (α-BiNbO₄). *Mater. Res. Bull.*, 28, 523–529.
13. West, A.R. & Andres-Verges, M. (1997). Impedance and modulus spectroscopy of ZnO varistors. *J. Electroceram.*, 1(2), 125–132.
14. Irvine, J.T.S., Sinclair, D.C. & West, A.R. (1990). Electroceramics: Characterization by impedance spectroscopy. *Adv. Mater.*, 2(3), 132–138.
15. Nobre, M.A.L. & Lanfredi, S. (2003). Dielectric spectroscopy on Bi₃Zn₂Sb₃O₁₄ ceramic: An approach based on the complex impedance. *J. Phys. Chem. Solids*, 64, 2457–2464.
16. Jonscher, A.K. (1997). The 'universal' dielectric response. *Nature*, 267, 673–679.
17. Herbert, J.M. (1985). The properties of dielectrics. In D.S. Cambell (Ed.). *Ceramics dielectrics and capacitors*. Amsterdam: Gordon and Breach Science Publishers S.A., 9–62.